Reliable Detection of Transmit-Antenna Number for MIMO Systems in Cognitive Radio-Enabled Internet of Things

Junlin Zhang, Mingqian Liu, *Member, IEEE*, Ning Zhang, *Senior Member, IEEE*, Yunfei Chen, *Senior Member, IEEE*, Fengkui Gong, *Member, IEEE*, Qinghai Yang, *Member, IEEE*, and Nan Zhao, *Senior Member, IEEE*

***Abstract*—Identification of transmit-antenna number is of importance in cognitive Internet of Things with multiple-input multiple-output (MIMO). Previous studies on transmit-antenna number detection only consider Gaussian noise and ignore impulsive interference. In the practical wireless communication, impulsive interference may exist due to low-frequency atmospheric noise, multiple access and electromagnetic disturbance. Such interference can usually be modeled as symmetric alpha stable ($S\alpha S$), which cause the performance degradation of conventional algorithms based on Gaussian model. In this paper, we present a novel scheme to detect the transmit-antenna number for MIMO systems in cognitive Internet of Things, assuming that signals are corrupted by both $S\alpha S$ interference and Gaussian noise. We first introduce a new approach to characterize the generalized correlation matrix, and provide its bound with $S\alpha S$ interference. Then, the discriminating feature vector is constructed by utilizing the higher-order moments (HOM) of eigenvalues of the generalized correlation matrix. Finally, an advanced clustering algorithm is employed to detect the transmit-antenna number, using the cluster where the minimum eigenvalue is located. The proposed algorithm avoids the need for a priori information about the transmitted signals, such as coding mode, modulation type and pilot patterns. Simulation experiments demonstrate the feasibility of the proposed transmit-antenna number detection scheme in MIMO systems with Gaussian noise and $S\alpha S$ interference.**

***Index Terms*—Alpha-stable interference, cognitive radio, Internet of Things, number of transmit antennas, parameter identification.**

I. Introduction

THE INTERNET of Things (IoT) has recently attracted much attention due to its wide range of applications, such as environmental, industrial, biomedical sensing and monitoring [1], [2]. Meanwhile, cognitive IoT (CIoT) becomes important by equipping the IoT network with cognition. CIoT enables IoT devices to learn and make intelligent decisions by sensing the physical and social environments [3], [4]. To achieve intelligent transmission, identification of signal parameters is a key requirement, such as detection of transmit-antenna number and classification of space-time code [5], [6]. In particular, antenna enumeration is an important task for CIoT, which helps to improve the coexistence of the primary users (PUs) and secondary users (SUs). In other words, the knowledge about the transmit-antenna number for PUs enables SUs to modify the transmit power and beamforming to achieve coexistence between PUs and SUs [7], [8]. Moreover, detection of the transmit-antenna number plays an important role in antenna selection techniques, which avoid overhead and transmission delay caused by additional signaling [8]. Thus, the identification of transmit-antenna number should be carefully considered in CIoT.

Several schemes for detecting problem of the transmit-antenna number have been presented in the literature. Previous works can be roughly divided into two categories: information-theoretic (ITC) and hypothesis testing based (HT) approaches. The ITC approaches detect the number of transmit antennas by determining the rank of the covariance matrix (CM) of the received signals. The HT approaches make a decision based on multiple hypothesis testing, which exploit the distribution of the eigenvalues of the covariance matrix to design a test statistic and threshold. For example, the ITC, including Akaike information criterion (AIC) and minimum description length (MDL) criterion, were applied to detect the transmit-antenna number in [9], [10]. It does not need to track the eigenvalues of the sample CM, and thus avoid high computational complexity. Moreover, the performance of the adaptive estimator was dependent on the receive-antenna number of MIMO systems. K. Hassan, *et al*. [11] investigated the problem of identification of transmit-antenna numbers for spatially-correlated MIMO and proposed two algorithms based on objective information theoretic criteria. These two algorithms are robust to the spatial correlation of the channel, but their performance is vulnerable to timing and frequency offsets.

In HT algorithm, the basic idea is to obtain the dimension of noise eigenvalue of the sample CM. Oularbi *et al*. proposed a multiple-hypothesis testing scheme to identify the number of transmit antennas of the base station [12]. This scheme exploited the orthogonality of pilot pattern for different transmit

This work was supported by the National Natural Science Foundation of China under Grant 62071364, in part by the Aeronautical Science Foundation of China under Grant 2020Z073081001, in part by the Fundamental Research Funds for the Central Universities under Grant JB210104, and in part by the 111 Project under Grant B08038. *(Corresponding author: Mingqian Liu.)*

J. Zhang, M. Liu, F. Gong and Q. Yang are with the State Key Laboratory of Integrated Service Networks, Xidian University, Shaanxi, Xi'an 710071, China (e-mail: zhangjl@stu.xidian.edu.cn; mqliu@mail.xidian.edu.cn; fkgong@xidian.edu.cn; qhyang@xidian.edu.cn).

N. Zhang is with the Department of Electrical and Computer Engineering, University of Windsor, Windsor, Canada (e-mail: ning.zhang@uwindsor.ca).

Y. Chen is with the School of Engineering, University of Warwick, Coventry, West Midlands United Kingdom of Great Britain and Northern Ireland CV4 7AL (e-mail: Yunfei.Chen@warwick.ac.uk).

N. Zhao is the School of Information and Communication Engineering, Dalian University of Technology, Dalian 116024, China (e-mail: zhaonan@dlut.edu.cn).

antennas as a discriminating features to detect the transmit-antenna number. Mohammadkarimi *et al*. in [13] developed a multiple hypothesis testing-based algorithm that exploited the higher order statistics of the signal and the characteristic of time-varying channel in MISO system. In [14], Li *et al* presented two detection algorithms. one relies on the ratio of the maximum eigenvalue to the sum of eigenvalues; the other is based on the distribution properties of the second-order moment (SOM) of the Wishart matrix. Li *et al*. [15] developed a new HT-based estimator, using the statistical properties of HOM of the sample CM eigenvalues, to detect the transmit-antenna number for MIMO systems. In addition, the problem of detecting the transmit-antenna number was addressed for the MIMO orthogonal frequency division multiplexing by extending the ITC and HT approaches [16], [17].

Previous works on antenna enumeration have assumed that the noise is Gaussian. However, a wide variety of man-made and physical interference exhibit impulsive behavior in practice. Examples include the multiple access/co-channel interference, atmospheric interference or shallow underwater interference [18], [19]. For impulsive interference, the family of alpha-stable distributions has provided an accurate model [20]. Since alpha-stable processes with infinite variance, existing methods based on covariance exhibit considerable performance degradation. Although several schemes have been proposed in the literature for the alpha-stable noise/interference, such as Myriad filter [21], fractional lower-order statistics [22], zero order statistics [23], correntropy [24] and nonlinear preprocessor [25]. To the best of our knowledge, no work exists in the literature on antenna enumeration in MIMO systems with Gaussian noise and $S\alpha S$ interference.

In this paper, we develop a novel scheme to detect the transmit-antenna number for MIMO transmissions with Gaussian noise and $S\alpha S$ interference. First, a novel approach is introduced to characterize the generalized correlation matrix, and the boundedness and the particular structure of the generalized correlation matrix are provided for $S\alpha S$ interference. Then, a discriminating feature vector is calculated relying on the higher-order moment of the eigenvalues of the generalized correlation matrix. Furthermore, we propose a detection scheme using adaptive cluster forests to achieve better identification performance. The scheme has the advantage that it avoids the need for a priori information about system parameters and pilot patterns.

The main contributions of this paper are described as follows.

- To the best of our knowledge, it is the first work that detects the number of transmit antennas for MIMO systems with Gaussian noise and $S\alpha S$ interference, while previous works only consider Gaussian noise.
- We introduce the generalized correlation matrix and analyze its boundedness and particular structure. Moreover, a novel scheme is proposed to detect the transmit-antenna number by employing the generalized correlation matrix and adaptive cluster forests. This is the first time that the generalized correlation matrix and clustering algorithm are used in transmit-antenna number detection.
- The proposed scheme shows the superiority over the existing algorithms when both Gaussian noise and $S\alpha S$ interference are present. Furthermore, the proposed scheme does not require prior knowledge about the pilot patterns and preamble sequence.

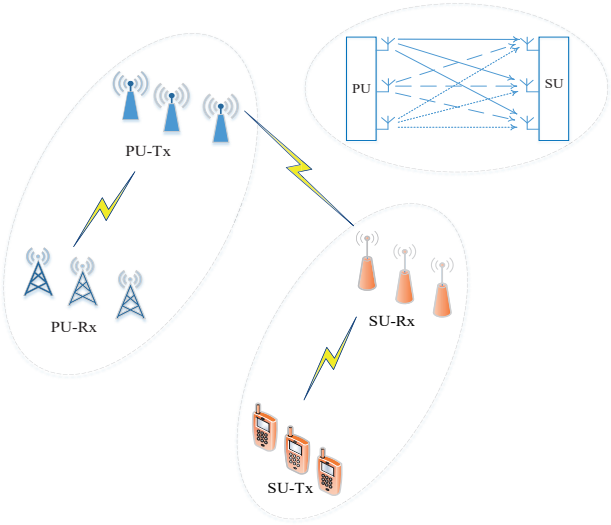

Fig. 1. System model for CIoT

The remainder of the paper is structured as follows. In Section II, the system model and relevant works are presented. The generalized correlation matrix is introduced in Sections III. The proposed detection scheme is reported in Sections IV. Simulation results are discussed in Section V, and some conclusions are drawn in Section VI.

II. System Model and Preliminaries

A. System Model

Consider a typical CIoT system where the SU needs to detect the number of PU transmit antennas. A typical scenario is illustrated in Fig. 1. In CIoT, we assume a MIMO communication system employing M_t transmit antennas and M_r receive antennas ($M_r > M_t$). This configuration corresponds to an IoT device with multiple antennas. The SU has no prior information about the transmit-antenna number of PU. The modulated symbols are come from the M-point constellation $\mathbb{M}$, e.g., M=4 for $\mathbb{M}$= 4-PSK, M=8 for $\mathbb{M}$= 8-PSK, M=16 for $\mathbb{M}$=16-QAM and M=64 for $\mathbb{M}$=64-QAM. This paper assumed the flat-fading MIMO channel characterized by an $M_r \times M_t$ matrix of Rayleigh fading coefficients. Under these assumptions, the received signal at the m-th antenna of SU can be described as

$$\begin{aligned} r_m(n) &= \tilde{s}_m(n) + I_m(n) + w_m(n) \\ &= \sum_{q=1}^{M_t} h_{mq} s_q(n) + I_m(n) + w_m(n), \end{aligned} \tag{1}$$

where $s_q(n)$ is the transmitted samples at the q-th transmit antenna of PU, $I_m(n)$ is the impulsive interference at the m-th receive antenna, $w_m(n)$ is the Gaussian noise at the m-th receive antenna and h_{mq} represents the Rayleigh fading channel coefficient between the q-th transmit antenna and m-th

TABLE I
NOTATIONS.

Notations	Descriptions	Notations	Descriptions
$[\cdot]^T$	Transposition	$\lvert\cdot\rvert$	Absolute value
$(\cdot)^\dagger$	Hermitian transpose	$(\cdot)^*$	Complex conjugate
$E\{\cdot\}$	Mathematical expectation	$\mathrm{diag}(\cdot)$	Diagonal matrix
$\log(\cdot)$	Logarithmic function	$\exp(\cdot)$	Exponential function
$tr(\cdot)$	Trace operator	$\lVert\cdot\rVert_F$	Frobenius norm
δ	Kronecker delta	e	Euler's constant
$\mathrm{Re}\{\cdot\}$	Real part	$\mathrm{Im}\{\cdot\}$	Imaginary part
$\neq$	Not equal sign	$\simeq$	Approximately equal sign

receive antenna. The $M_r \times 1$ observation vector at the receiver, i.e., $\mathbf{r}(n) = [r_1(n), ..., r_{M_r}(n)]^T$, is expressed as

$$\mathbf{r}(n) = \mathbf{H}\mathbf{s}(n) + \mathbf{I}(n) + \mathbf{w}(n), \tag{2}$$

where $\mathbf{H}$ corresponds to the $M_r \times M_t$ complex matrix of i.i.d. flat Rayleigh fading channels, $\mathbf{w}(n) = [w_1(n), ..., w_{M_r}(n)]^T$ represents the Gaussian noise with variance σ_n^2 and $\mathbf{I}(n) = [I_1(n), ..., I_{M_r}(n)]^T$ is the $M_r \times 1$ impulsive interference vector. The impulsive interference $I_i(n)$ follows an $S\alpha S$ distribution, which is often characterized by its characteristic function as

$$\varphi(u) = \exp\{j\tilde{e}u - \gamma_\alpha |u|^\alpha\}. \tag{3}$$

The characteristic exponent α determines the impulsiveness, and a smaller α leads to a more impulsive behavior. The scale parameter γ_α controls the spread of the distribution and $\tilde{e}$ is the location parameter that represents the mean for $2 \geq \alpha > 1$.

B. Relevant Works

We briefly review several typical detection algorithms, which will be used in the sequel as the bases for comparison with our proposed detection scheme.

1) WME Algorithm: The algorithm exploits the precise distribution of the test statistic based on the eigenvalue of the Wishart matrix, and determines the number of transmit antennas according to hypothesis test [14]. The test statistic can be expressed as

$$U_k = \frac{l_k}{\frac{1}{M_r-k+1}\sum_{j=k}^{M_r} l_j}, \tag{4}$$

where l_k is the k-th eigenvalue of the sample CM.

Relying on the random matrix theory, the distribution function of U_{M_t+1} can be given by

$$\begin{aligned} &P\left\{\frac{U_{M_t+1} - \mu^U_{M_r-M_t,N}}{\varepsilon^U_{M_r-M_t,N}} \leq x\right\} \approx F(x) \\ &= F_{W_2}(x) - \frac{1}{2(M_r-M_t)N}\left(\frac{\mu^U_{M_r-M_t,N}}{\varepsilon^U_{M_r-M_t,N}}\right)^2 F''_{W_2}(x), \end{aligned} \tag{5}$$

where $F_{W_2}(\cdot)$ is the Tracy-Widom distribution function of order 2 and $F''_{W_2}(\cdot)$ is second derivative of $F_{W_2}(\cdot)$. $\mu^U_{m,n}$ and $\varepsilon^U_{m,n}$ are centering and scaling parameters as

$$\begin{cases} \mu^U_{m,n} = \left(\sqrt{\frac{m}{n}} + 1\right)^2 \\ \varepsilon^U_{m,n} = n^{-2/3}\left(\sqrt{\frac{m}{n}} + 1\right)\left(\sqrt{\frac{n}{m}} + 1\right)^{1/3}. \end{cases} \tag{6}$$

The threshold γ_k^U can be given by

$$\phi_k^U = F^{-1}(1 - P_f)\,\varepsilon^U_{N_r-k+1,N} + \mu^U_{N_r-k+1,N}, \tag{7}$$

where $F^{-1}(\cdot)$ denotes the inverse of $F(\cdot)$ defined in (5) and P_f is the false-alarm probability. When $U_k \leq \phi_k^U$, then l_k is classified as a noise eigenvalue. The final identification result is $M_t = k - 1$.

2) SM-PET Algorithm: The SM-PET algorithm can be regarded as an extension of the predicted eigenvalue threshold (PET) algorithm. This algorithm employs the distribution functions of the SOM eigenvalues to derive the one-step predicted upper bound [14]. The SOM eigenvalues can be expressed as

$$T_{M_r-k+1} = \frac{1}{k}\sum_{j=M_r-k+1}^{M_r} l_j^2. \tag{8}$$

The predicted upper bound can be given by

$$\phi^l_{M_r-k} = \sqrt{((k+1)\,\mathrm{R} - k)\,T_{M_r-k+1}}, \tag{9}$$

where R is given by (10) shown at the top of the next page. The decision rule is that the number of transmit antennas is $M_r - k$ when $l_{M_r-k} > \phi^l_{M_r-k}$.

3) HOM-HT Algorithm: This algorithm utilizes the distribution properties of the HOM eigenvalues to obtain the test statistics features [15]. It exploits a serial binary hypothesis test to detect the transmit-antenna number. The test statistics based on the HOM eigenvalues can be expressed as

$$U_r(k) = \frac{1}{M_r - k}\sum_{j=k+1}^{M_r} \frac{l_j^r}{\hat{\sigma}^{2r}(k)}, \tag{11}$$

$\hat{\sigma}^2$ is the estimate of the noise variance, using the maximum likelihood method, which can be given by

$$\hat{\sigma}^2(k) = \frac{1}{M_r - k}\sum_{j=k+1}^{M_r} l_j. \tag{12}$$

$$\mathrm{R}=\frac{\sqrt{Nk\left(k+1\right)}\left(N+\left(k+1\right)\right))+t\sqrt{2k\left(2(k+1)^{2}+5N\left(k+1\right)+2N^{2}\right)}}{\sqrt{Nk\left(k+1\right)}\left(N+k\right)-t\sqrt{2\left(k+1\right)\left(2k^{2}+5Nk+2N^{2}\right)}}. \tag{10}$$

The threshold ϕ_r can be given by

$$\phi_r=\alpha_r+t\sqrt{\frac{\beta_r}{M_r^2}}, \tag{13}$$

where α_r and β_r are mean and covariance of $U_r\left(k\right)$. When $U_r\left(k\right)\leq\phi_r$, $\hat{M}_t=k$.

III. Generalized Correlation Matrix

The second-order statistics, i.e., the correlation matrix and second-order moment, have been widely used to detect the transmit-antenna number. However, they are not suitable for the impulsive interference, as their variances do not exist or go to infinity [21]. Thus, the observation signal in (2) is corrupted by $S\alpha S$ interference, which makes its variance go to infinity, although the Gaussian noise has finite variance. One has to utilize the fractional lower order statistics (FLOS) to characterize the behavior of impulsive interference [22]. While FLOS is feasible in the characterization and processing of impulsive noise/interference, it does not provide a generic framework for tackling the impulsive noise/interference. $S\alpha S$ interference exhibits finite absolute moments only when the order of the moment is less than the characteristic exponent, that is $p<\alpha$. Thus, the values of p need to be restricted in the valid interval, which requires a priori information about α. A priori information is unrealistic in many practical applications, while estimation may be inaccurate and/or computationally intensive [23].

In this paper, we develop a generalized correlation matrix (GCM) as an approach to statistical correlation characterization, which is well-defined overall distributions for impulsive behavior. The GCM is based on the compression function of the form. The GCM of the received signals can be defined as

$$\begin{aligned}\mathbf{G_r}&=E\left\{\overleftrightarrow{\mathbf{r}}\left(n\right)\overleftrightarrow{\mathbf{r}}^{\dagger}\left(n\right)\right\}\\&=\begin{bmatrix}G_{11}&\cdots&G_{1M_r}\\\vdots&\ddots&\vdots\\G_{M_r1}&\cdots&G_{M_rM_r}\end{bmatrix},\end{aligned} \tag{14}$$

where $\overleftrightarrow{\mathbf{r}}\left(n\right)=\left[\frac{r_1(n)}{f[r_i(n)]},\cdots,\frac{r_{M_r}(n)}{f[r_{M_r}(n)]}\right]$ can be given by

$$G_{im}=E\left\{r_i\left(n\right)\frac{r_m^{*}\left(n\right)}{f\left[r_i\left(n\right)\right]f\left[r_m\left(n\right)\right]}\right\}, \tag{15}$$

where $f\left[r_i\left(n\right)\right]=\left|r_i\left(n\right)\right|+\left|\vartheta\right|$ when $\left|r_i\left(n\right)\right|>\zeta\left(n\right)$ and $f\left[r_i\left(n\right)\right]=1$ otherwise. $\zeta\left(n\right)=3\tau_Q\left(n\right)$, $\tau_Q\left(n\right)$ is the midpoint element of the order statistic of $\left|r_i\left(n\right)\right|$ and $\left|\vartheta\right|\to 0$. $r_i\left(n\right)$ and $r_m\left(n\right)$, $\forall i$, $\forall m$, are the received signal defined in Section II.

Let us first study the boundedness of GCM $\mathbf{G_r}$.

Proposition 1: The GCM $\mathbf{G_r}$ is bounded, i.e., the (i,m)-th entry G_{im} is bounded as

$$-\infty<G_{im}=E\left\{r_i\left(n\right)\frac{r_m^{*}\left(n\right)}{f\left[r_i\left(n\right)\right]f\left[r_m\left(n\right)\right]}\right\}<\infty. \tag{16}$$

Proof: See Appendix A. ∎

Proposition 1 provides the boundedness of GCM, which is the foundation for the detection of transmit-antenna number in $S\alpha S$ interference.

A particular structure of the GCM is shown in Proposition 2, which is helpful for the detection of transmit-antenna numbers.

Proposition 2: The generalized correlation matrix $\mathbf{G_r}$ can be expressed as

$$\mathbf{G_r}=\mathbf{H\Sigma H}^{\dagger}+\varpi^2\mathbf{I}, \tag{17}$$

and the (i,m)-th entry G_{im} can be given by

$$G_{im}\simeq\sum_{q=1}^{M_t}h_{iq}\Sigma_{qq}h_{mq}^{*}+\varpi_w^2\delta_{im}, \tag{18}$$

where

$$\Sigma_{qm}\simeq\delta_{qm}E\left\{\frac{s_q(n)\left(\sum\limits_{q=1}^{M_t}s_q(n)+I_m(n)+w_m(n)\right)}{f\left[r_i\left(n\right)\right]f\left[r_m\left(n\right)\right]}\right\}, \tag{19}$$

$$\varpi^2=E\left\{\frac{\left(I_i(n)+w_i(n)\right)\left(\sum\limits_{q=1}^{M_t}h_{mq}s_q(n)+I_m(n)+w_m(n)\right)}{f\left[r_i\left(n\right)\right]f\left[r_m\left(n\right)\right]}\right\}, \tag{20}$$

and δ_{qm} is the Kronecker delta.

Proof: See Appendix B. ∎

Proposition 2 reveals that $\mathbf{G_r}$ includes M_t information. $\mathbf{G_r}$ is a nonnegative definite Hermitian matrix, which can be decomposed as

$$\mathbf{G_r}=\mathbf{U\Lambda U}^{\dagger}, \tag{21}$$

where $\mathbf{U}$ is a unitary matrix with $M_r\times M_r$ and $\mathbf{\Lambda}$ is an nonsingular covariance matrix that stacks all the eigenvalues of $\mathbf{G_r}$,

$$\mathbf{\Lambda}=\mathrm{diag}\left(\lambda_1,\lambda_2,\cdots,\lambda_{M_t},\lambda_{min},\cdots,\lambda_{min}\right), \tag{22}$$

where λ_{min} is the smallest eigenvalue and their multiplicity is M_r-M_t. In such a case, we denote the eigenvalues of $\mathbf{G_r}$ by

$$\lambda_1\geq\lambda_2\geq\cdots\geq\lambda_{M_t}\geq\lambda_{M_t+1}=\cdots\lambda_{M_r}. \tag{23}$$

From (23), the eigenvalues of $\mathbf{G_r}$ include the information of transmit antennas M_t, which can be detected by determining the multiplicity order of the smallest eigenvalue of $\mathbf{G_r}$. In

practice, we have to estimate $\mathbf{G_r}$ from the finite number of received signals, which can be performed as

$$\hat{\mathbf{G}}_{\mathbf{r}} = \begin{bmatrix} \hat{G}_{11} & \cdots & \hat{G}_{1M_r} \\ \vdots & \ddots & \vdots \\ \hat{G}_{M_r1} & \cdots & \hat{G}_{M_rM_r} \end{bmatrix}, \tag{24}$$

and $\hat{G}_{im}$ is the (i,m)-th entry of $\hat{\mathbf{G}}_{\mathbf{r}}$,

$$\hat{G}_{im} = \frac{1}{N}\sum_{n=1}^{N} r_i(n)\frac{r_m^*(n)}{f[r_i(n)]\,f[r_m(n)]}. \tag{25}$$

Let the eigenvalues of $\hat{\mathbf{G}}_{\mathbf{r}}$ be

$$\ell_1 \geq \ell_2 \geq \cdots \ell_{M_t} \geq \ell_{M_t+1} \geq \cdots \geq \ell_{M_r}, \tag{26}$$

and the smallest eigenvalues ℓ_{M_r} are different from the smallest eigenvalues λ_{min} in (23), and the multiple order of ℓ_{M_r} is not $M_r - M_t$. This is mainly because the theoretical value of the eigenvalues λ_{min} is deviated from the estimated value ℓ_{min} for small sample N. Obviously, it is infeasible to achieve antenna enumeration by observing the smallest eigenvalue of $\hat{\mathbf{G}}_{\mathbf{r}}$ directly.

IV. Proposed Detection Algorithm for Transmit Antenna Number

Detection of the transmit-antenna number employed in the MIMO system can be converted into determining the multiplicity order of the smallest eigenvalue of $\mathbf{G_r}$ of the $M_r \times 1$ received signals. When N is large, i.e., $N \to \infty$, the smallest $M_r - M_t$ eigenvalues are equal to the noise power. Thus, the dimension of the noise subspace is $M_r - M_t$, whereas the remaining M_t eigenvalues represent the signal subspace. In practice, the boundary between the noise and signal eigenvalues is indistinguishable due to the sample scarcity, leading to degradation in the detection performance. To overcome this, the HT algorithm, using higher-order moments of eigenvalues, can be an excellent solution to the problem of the spread of the eigenvalues [15]. However, HT-based detection methods require the construction of test statistics and the derivation of the test threshold relied on the distributional properties of the test statistics, which are difficult to obtain. Consequently, the detection threshold cannot be derived. To overcome these limitations, we transform the problem of detecting the transmit-antenna number into determining the number of clustering elements. Then, an advanced clustering algorithm is used to classify the discriminant feature vector, which distinguishes the cluster of noise eigenvalues and signal eigenvalues. Furthermore, the transmit-antenna number can be estimated from the number of elements L_n for the cluster of noise eigenvalues as $\hat{M}_t = M_r - L_n$.

Here, we employ the higher-order moments of the eigenvalues of GCM to construct a discriminating feature vector. We first construct a pair of test statistics as

$$T_k^a = \lg\left(\frac{\overline{\eta_k^r}}{\frac{1}{M_r-k}\sum_{j=k+1}^{M_r}\eta_j}\right), \tag{27}$$

$$T_k^b = \lg\left(\frac{\overline{\eta_k^r}}{\left(\prod_{j=k+1}^{M_r}\eta_j\right)^{1/(M_r-k)}}\right), \tag{28}$$

where $\overline{\eta_k^r} = \frac{1}{M_r-k}\sum_{j=k+1}^{M_r}\eta_j^r$ and

$$\eta_k = \frac{(\Delta_k - \omega_k)}{2\omega_k}\Delta_k, \tag{29}$$

in which $\Delta_k = \frac{D_n \ell_k}{\frac{1}{M_r}\sum_{i=1}^{M_r}\ell_i}$ $(k = 1, 2, \cdots M_r - 1)$ and $\Delta_{M_r} = \Delta_{M_r-1}$. $D_n = log(N/M_r)$ and $\omega_k = \frac{1}{M_r-k+1}\sum_{j=k}^{M_r}\Delta_j$.

Then, the discriminating feature vector can be expressed as

$$\mathbf{\Psi} = [\Psi_1(k), \Psi_2(k)], \tag{30}$$

where $\mathbf{\Psi}$ is discriminating feature vector, $\Psi_1(k) = \mathrm{Im}\{\log_2(T_k^a)\} + \mathrm{Im}\{\log_2(T_k^b)\}$ and $\Psi_2(k) = \mathrm{Re}\{\log_2(T_k^a)\} + \mathrm{Re}\{\log_2(T_k^b)\}$.

A. Adaptive Cluster Forests

Cluster ensemble is a powerful tool to integrate multiple clustering solutions for higher accuracy. Typically, there are two major stages in cluster ensemble approaches, i.e., the ensemble generation and the consensus aggregation. In the first stage, a wider variety of basic clustering are generated in the ensemble. The objective of the second stage is to find a consensus function to integrate the basic clustering, which can achieve more accurate and stable clustering results [26].

In this paper, an adaptive cluster forests (ACF) clustering is employed, which combines the improved spectral clustering algorithm and fuzzy clustering algorithm [27]. The algorithm first discards redundant and irrelative features and estimates fuzzy exponent value by using unsupervised feature selection based ς value. Then, for the selected feature vector, fuzzy C-means clustering based on estimated fuzzy exponent value is used to obtain the clustering vector label. Subsequently, the pseudo clustering results are utilized to generate co-cluster matrices. Finally, the final vector labels are obtained by employing the spectral clustering algorithm to cluster the computed regularized co-cluster matrix [27].

In the following, we will briefly explain two clustering techniques, which will be employed in the proposed method.

1) Fuzzy C-Means clustering: FCM clustering is developed based on fuzzy theory, which provides more flexible clustering results. The algorithm realizes clustering by optimizing the objective function, which calculates the degree of membership of each data example to each cluster center [28]. The FCM objective function as

$$J_m = \sum_{i=1}^{c}\sum_{j=1}^{K}(\mu_{ij})^m \times d_{ij}(x_j, \theta_i), \tag{31}$$

where $\mu_{ij} \in [0,1]$, $\sum_{i=1}^{c} \mu_{ij} = 1$ and $0 < \sum_{i=1}^{K} \mu_{ij} < K$. $d_{ij}\left(x_j, \theta_i\right)$ is the distance between the data x_i and the center of the cluster θ_j as

$$d_{ij}\left(x_j, \theta_i\right) = \left(x_j - \theta_i\right)^T I \left(x_j - \theta_i\right). \tag{32}$$

μ_{ij} is provided as (33) at the next page, where $\theta_i = \frac{\sum_{j=1}^{K} \left(\mu_{ij}\right)^m x_j}{\sum_{j=1}^{K} \left(\mu_{ij}\right)^m}$.

Fuzzy clustering can truly reflect the actual relationship of object data based on fuzzy theory, but it is sensitive to the difference of data distribution. Spectral clustering is more adaptable to the difference of data distribution, and its computational complexity is small.

2) Spectral clustering algorithm: Spectral clustering is considered superior to traditional clustering algorithms by modeling arbitrary shaped clusters [29].

Let $\mathcal{G}\left(\mathcal{X}, \mathcal{A}\right)$ be a weighted undirected graph, where $\mathcal{X}$ represents a vertex set and $\mathcal{A}$ is the associated affinity matrix. $\mathcal{A}$ is symmetric and non-negative, whose entry $\mathcal{A}_{ij}$ denotes the similarity between samples

$$\mathcal{A}_{ij} = \begin{cases} \exp\left(-\frac{\|y_i - y_j\|^2}{\upsilon^2}\right) & y_i \text{ and } y_j \text{ areneighbors} \\ 0 & \text{otherwise}, \end{cases} \tag{34}$$

where υ is the spread parameter. For the adjacency matrix $\mathcal{A}$ at each time instance, the corresponding degree matrix is a diagonal matrix $\mathcal{D} = \operatorname{diag}\left(\mathcal{D}_{11}, , \mathcal{D}_{ZZ}\right)$ with

$$\mathcal{D}_{ii} = \sum_{j=1}^{Z} \mathcal{A}_{ij}. \tag{35}$$

Then, the Laplacian graph $\mathcal{L}$ can be defined by $\mathcal{L} = \mathcal{D} - \mathcal{A}$. Let $tr\left(\mathcal{A}\right)$ be the trace operator of matrix $\mathcal{A}$. The minimization of the normalized cut criterion can be transformed into [29]

$$\max_{\mathcal{Z}^T \mathcal{D} \mathcal{Z} = I_c} tr\left(\mathcal{Z}^T \mathcal{A} \mathcal{Z}\right), \tag{36}$$

where I_c is the identity matrix and $\mathcal{Z} = \mathcal{B}\left(\mathcal{B}^T \mathcal{D} \mathcal{B}\right)^{-1/2}$. Given a scaled cluster assignment matrix $\mathcal{F}$, the objective function (36) can be rewritten as

$$\max_{\mathcal{F}^T \mathcal{F} = I_c} tr\left(\mathcal{F}^T \mathcal{D}^{-\frac{1}{2}} \mathcal{A} \mathcal{D}^{-\frac{1}{2}} \mathcal{F}\right), \tag{37}$$

where

$$\mathcal{F} = \mathcal{D}^{\frac{1}{2}} \mathcal{Z} = \mathcal{D}^{\frac{1}{2}} \mathcal{B}\left(\mathcal{B}^T \mathcal{D} \mathcal{B}\right)^{-\frac{1}{2}}. \tag{38}$$

To simplify the problem, the matrix $\mathcal{F}$ can be relaxed from the discrete values to continuous ones. The optimization to (37) can be rewritten as

$$\max_{\tilde{\mathcal{F}}^T \tilde{\mathcal{F}} = I_c} tr\left(\tilde{\mathcal{F}}^T \mathcal{V} \tilde{\mathcal{F}}\right), \tag{39}$$

where $\mathcal{V} = \mathcal{D}^{-1/2} \mathcal{A} \mathcal{D}^{-1/2}$. The optimal solution $\mathcal{F}$ of (39) can be found based on the eigenvalue of matrix $\mathcal{V}$.

B. Detection of the Transmit Antennas Number with Adaptive Cluster Forests

Based on the analysis above, the problem of detecting the transmit-antenna number is converted into the clustering from the discriminating feature vector, which is calculated via the higher-order eigenvalues of $\hat{\mathbf{G}}_{\mathbf{r}}$. Given that adaptive cluster forests is a powerful clustering algorithm, we will employ the adaptive cluster forests to make the decision on transmit antenna number. Following the procedure in [27], we first utilize the unsupervised feature selection step for the discriminating feature vector to remove noisy features and redundant features. Let ς be the validity index of the selected features, that is,

$$\varsigma = \frac{d_{WD}}{d_{BD}}, \tag{40}$$

where d_{WD} and d_{BD} are the within cluster distance and between cluster distance, respectively.

Then, the ensemble clustering based on multiple fuzzy C-Means clustering is employed to get a vector label as

$$\mathcal{RC} = \left\{rc_1, rc_2, \cdots, rc_{M_r - 1}\right\}, \tag{41}$$

where rc_i is the label of i-th feature vector. In this scheme, a dynamic estimation strategy is added to obtain the best fuzzy exponent value. The previous process is repeated.

Next, the clustering results of FCM-based ensemble clustering are used to create co-cluster matrices, which are summed and regularized. The feature selection algorithm stops when a termination condition is met as a number of features or a number of iterations. Finally, the spectral clustering algorithm is exploited to the computed regularized co-cluster matrices so as to get the final vector labels. The number of transmit antennas can be estimated as

$$\hat{M}_t = M_r - L_n. \tag{42}$$

where L_n is the dimension of the cluster for signal eigenvalues.

In conclusion, the main procedures of the proposed GCM-ACF algorithm is summarized in Algorithm 1.

Algorithm 1 Transmit-antenna number detection based on the GCM and ACF clustering

1: Compute the $\hat{\mathbf{G}}_{\mathbf{r}}$ of the received signal according to (24) and (25);
2: Obtain the eigenvalues ℓ_j of the matrix $\hat{\mathbf{G}}_{\mathbf{r}}$, and sort eigenvalues ℓ_j from large to small;
3: Construct the discriminating feature vector $\mathbf{\Psi}$ according to (30);
4: Obtain the vector of predicted clustering indices corresponding to the observations in the test statistic vector and the final centroid positions by using ACF clustering;
5: Determine the number of noise eigenvalues L_n based on the cluster in which the smallest eigenvalue is located;
6: Identify the transmit-antenna number $\hat{M}_t = M_r - L_n$.

$$\mu_{ij} = \begin{cases} \left[\sum_{\hbar=1}^{c} \left(\frac{d(x_j,\theta_i)}{d(x_j,\theta_\hbar)} \right)^{(2/(m-1))} \right]^{-1} & , \text{if } d\left(x_j, \theta_i\right) > 0 \\ 1 & , \text{if } d\left(x_j, \theta_i\right) = 0 \end{cases} \tag{33}$$

TABLE II
SIMULATION PARAMETERS.

Parameters	Default values
Modulation type	QPSK
MIMO channel	Flat Rayleigh fading
Space-time mode	STBC
Number of clusters	2
Number of clustering trees	20
Number of transmit-antenna	3
Order of eigenvalues r	10
Monte Carlo trials repeated	2000

V. SIMULATION RESULTS AND DISCUSSION

In this section, we conduct Monte Carlo simulation to validate the performance of the the proposed GCM-ACF scheme for the detection of transmit-antenna number with Gaussian noise and $S\alpha S$ interference. In the examples, the signal to interference ratio (SIR) is defined as SIR $= 10 \lg E\left[\|\mathbf{r}(n) - \mathbf{I}(n) - \mathbf{w}(n)\|_F^2\right] / (M_r \gamma_\alpha)$. In our simulation, we consider a MIMO system in CIoT networks. The linear space-time block coding is employed for multiple transmit antennas in MIMO communication. It is assumed that the received signal is affected by AWGN and $S\alpha S$ interference. The probability of detection, $P_d = \Pr\left[\hat{M}_t = M_t\right]$ is employed as a performance measure.

Fig. 2 presents the probability of detection P_d versus the SNR for $M_t = 3$, $M_t = 4$, and different orders of eigenvalues. We set the number of receiver antennas and received samples to $M_r = 10$ and $N = 400$, respectively. It is seen from Fig. 2 that the probability of detection P_d of the GCM-ACF scheme does not depend on the order of eigenvalues r. For different numbers of transmit antennas, the detection performance is not significantly improved, when the order r rises from 2 to 30. When SNR is 4dB and the probability of detection P_d is close to 99% for $M_t = 3$ and close to 92% for $M_t = 4$. Based on the results shown in Fig. 2, we set the order of eigenvalues as $r = 10$ in the subsequent simulation experiments.

Fig. 3 shows the performance of the GCM-ACF scheme for different numbers of clustering trees (Nct) in the ACF. The performance of the proposed method is hardly affected by the number of clustering trees. This is mainly because the discriminating feature vector have strong robustness.

In Fig.4, we investigate the performance of the GCM-ACF scheme for different numbers of receive antennas M_r. We set the number of transmit antennas and received samples to $M_t = 3$ and $N = 400$, respectively. From Fig. 4, it can be seen that the probability of detection P_d improves significantly

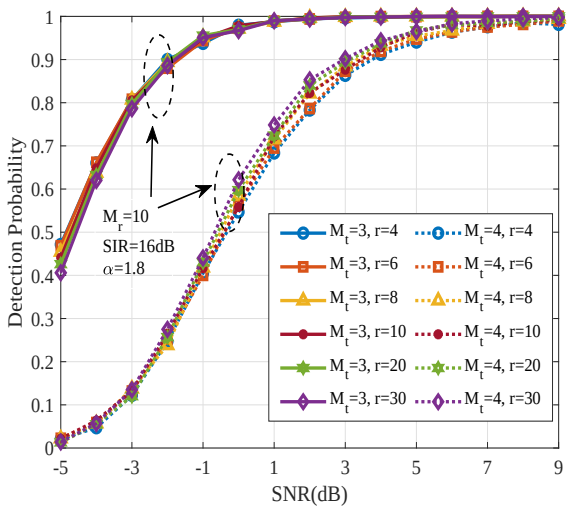

Fig. 2. Probability of correct detection, P_d, versus SNR for different orders of eigenvalues, for the GCM-ACF scheme with $M_r = 10$.

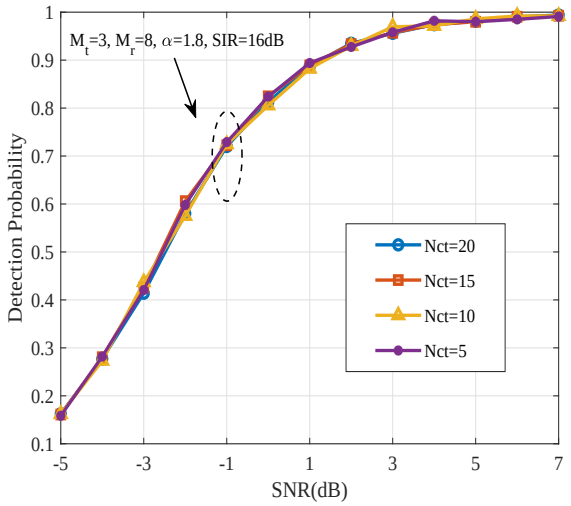

Fig. 3. Probability of correct detection, P_d, versus SNR for different numbers of clustering trees, for the GCM-ACF scheme with $M_t = 3$.

with increasing M_r. The main reason is that the number of receiver antennas improves the distinguish ability of the noise eigenvalues of $\hat{\mathbf{G}}_\mathbf{r}$.

In Fig. 5, the effect of the modulation schemes on the probability of detection P_d for the GCM-ACF scheme is shown. The numbers of transmit antennas, receiver antennas and received samples are set to $M_t = 3$, $M_r = 8$ and $N = 400$, respectively. According to Fig. 5, we can see that the performance of the GCM-ACF scheme is not affected by the modulation schemes. This is because the GCM-ACF scheme

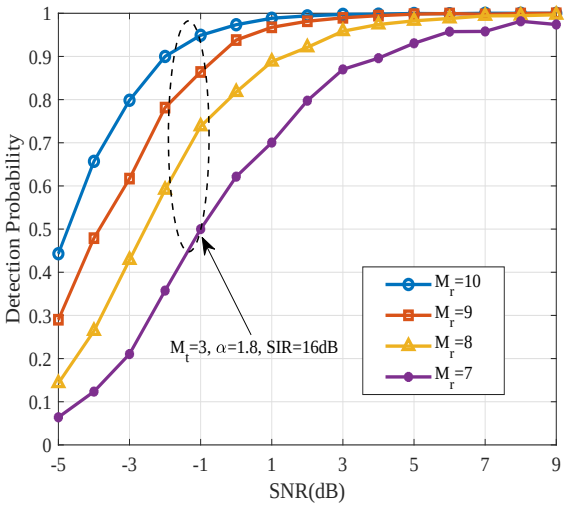

Fig. 4. Probability of correct detection, P_d, versus SNR for different numbers of receive antennas M_r, for the GCM-ACF scheme with $M_t = 3$.

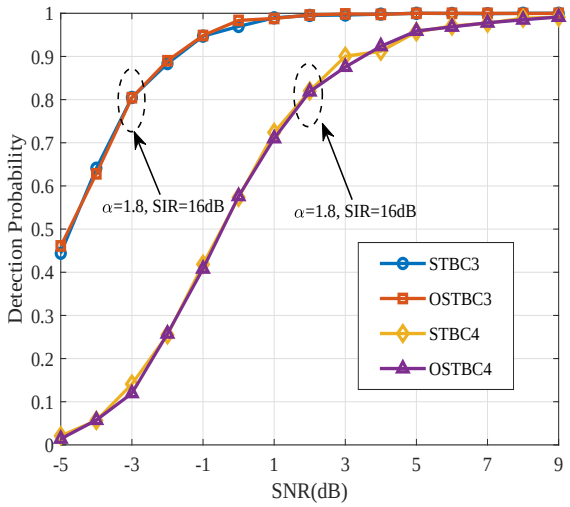

Fig. 6. Effect of the modulation schemes on P_d versus SNR for the GCM-ACF scheme with $M_t = 3$.

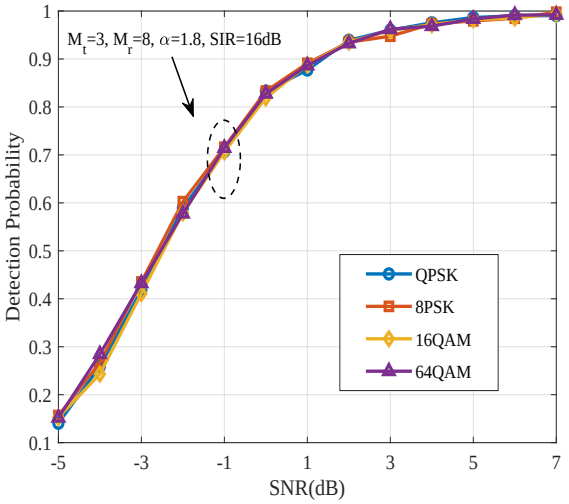

Fig. 5. Effect of the modulation schemes on P_d versus SNR for the GCM-ACF scheme with $M_t = 3$.

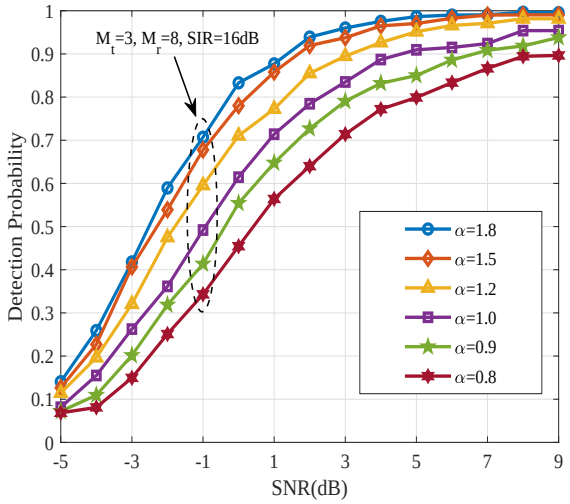

Fig. 7. Effect of the characteristic exponent α on P_d versus SNR for the GCM-ACF scheme with $M_t = 3$.

based on the $\hat{\mathbf{G}}_\mathbf{r}$ is independent of the modulation schemes.

Fig. 6 presents the probability of detection P_d of the algorithm for different space-time block codes. The space-time block codes under consideration are STBC3, OSTBC3, STBC4 and OSTBC4. We set the number of receiver antennas and received samples to $M_r = 10$ and $N = 400$, respectively. From the simulation results, it is clear that the probability of detection P_d is not dependent on the space-time block codes. This is because the feature vector is determined by the $\hat{\mathbf{G}}_\mathbf{r}$, which is independent of the space-time block codes. Note that a significant improvement of the proposed GCM-ACF scheme is caused by the difference numbers of transmit antennas in Fig. 6.

In Fig. 7, we depict the effect of the characteristic exponent α on the probability of correct detection P_d of the GCM-ACF scheme. The numbers of transmit antennas, receiver antennas and received samples are $M_t = 3$, $M_r = 8$ and $N = 400$, respectively. It is observed in Fig. 7 that, the performance of the GCM-ACF scheme degrades with decreasing the shape parameter α. For smaller α, the tails of $S\alpha S$ interference are the heavier which makes the noise eigenvalues of the $\hat{\mathbf{G}}_\mathbf{r}$ indistinguishable.

Fig. 8 demonstrates the influence of the SIR on the performance of the GCM-ACF scheme. We set the number of transmit antennas, receiver antennas and received samples are $M_t = 3$, $M_r = 8$ and $N = 400$, respectively. It can be observed that, with increasing SIR, the probability of detection P_d of the proposed GCM-ACF scheme improves because the effect of the $S\alpha S$ interference diminishes in $\hat{\mathbf{G}}_\mathbf{r}$.

Fig. 9 presents the effect of the number of received samples length N on the performance of the GCM-ACF scheme. We set the number of transmit antennas and receiver antennas are $M_t = 3$ and $M_r = 8$, respectively. It can be observed that, the probability of detection P_d of the proposed GCM-ACF

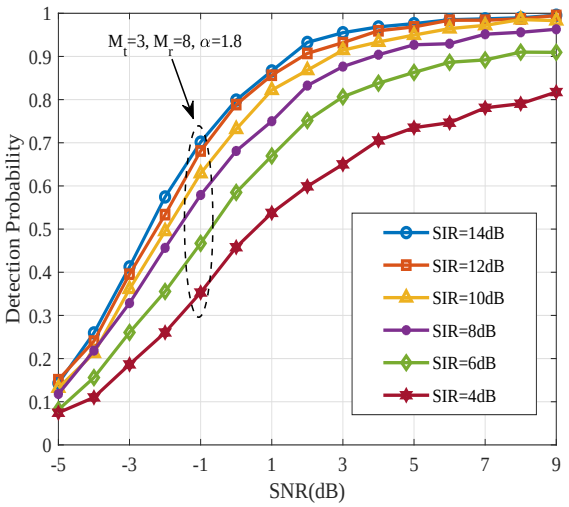

Fig. 8. Effect of the signal-to-interference ratio (SIR) on P_d versus SNR for the GCM-ACF scheme with $M_t = 3$.

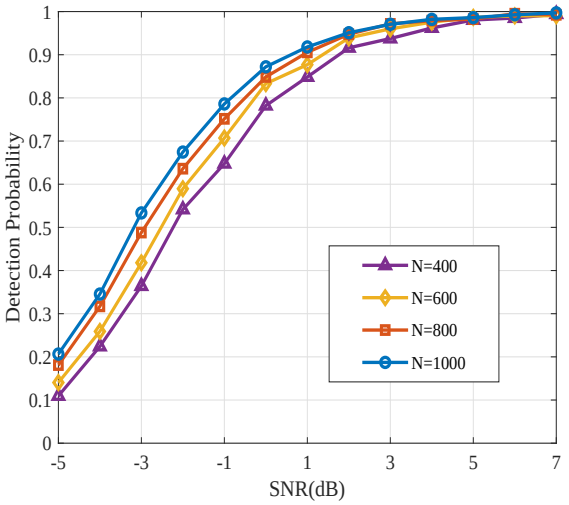

Fig. 9. Effect of received samples N on P_d versus SNR for the GCM-ACF scheme with $M_t = 3$.

scheme improves with increasing received samples N.

Fig. 10 compares the probability of detection P_d for the GCM-ACF algorithm, WME, SM-PET and HOM-HT. From Fig 10, it can be shown that the GCM-ACF scheme significantly outperforms the existing algorithms in and $S\alpha S$ interference. When SNR=4dB, the probability of detection P_d of the GCM-ACF scheme is close to 90%, while P_d of existing methods P_d is less than 15%. In addition, we show the probability of detection P_d of the number of transmit antennas under Gaussian noise in Fig. 10. The proposed method is still effective under Gaussian noise. According to the results, we conclude that the discriminating feature vector is robust to Gaussian noise and $S\alpha S$ interference. In addition, we evaluate the computational complexity of different algorithms. For the conventional WME, SM-PET and HOM-HT algorithms, the computational overhead comes mainly from the covariance matrix $O(M_r^2 N)$ and the eigenvalue decomposition $O(M_r^3)$.

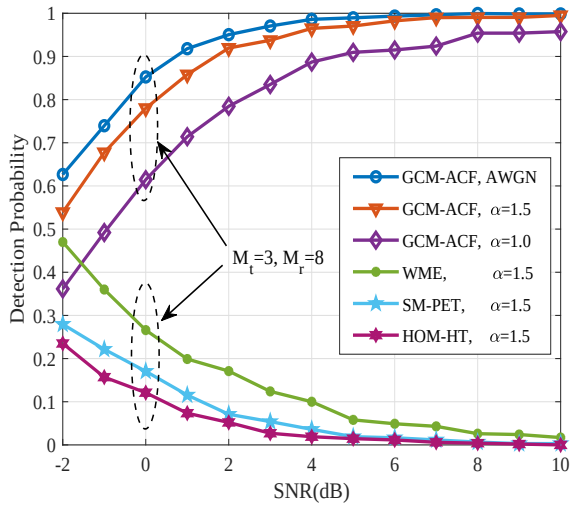

Fig. 10. Performance comparison of the GCM-ACF scheme and the WME, SM-PET and HOM-HT algorithm with $M_t = 3$.

For the GCM-ACF algorithm, the complexity of the discriminating feature vector comes from GCM $O(M_r^2 N)$ and EVD $O(M_r^3)$. Meanwhile, the proposed GCM-ACF algorithm requires an extra online clustering, whose complexity is mainly depended on FCM and SC. As a result, the proposed algorithm significantly showed higher computational complexity than the existing methods.

VI. Conclusion

This paper has developed a novel scheme based on the GCM of the received signal and ACF clustering to detect the transmit-antenna number in MIMO systems for CIoT. The number of transmit antennas has been detected relied on the number of noise eigenvalues, which was determined by the dimension of the cluster where the minimum eigenvalue is located. This scheme has the advantage of avoiding the need for a priori knowledge about the pilot patterns and system parameters. Simulation experiments have demonstrated that the proposed GCM-ACF algorithm can achieve a good performance Gaussian noise and $S\alpha S$ interference.

Appendix A
Proof of Proposition 1

G_{im} is can be expressed as

$$\begin{aligned} G_{im} &= \mathrm{Re}\left\{G_{im}\right\} + j\mathrm{Im}\left\{G_{im}\right\} \\ &= \mathrm{Re}\left\{E\left\{r_i(n)\frac{r_m^*(n)}{f\left[r_i(n)\right]f\left[r_m(n)\right]}\right\}\right\} \\ &+ j\mathrm{Im}\left\{E\left\{r_i(n)\frac{r_m^*(n)}{f\left[r_i(n)\right]f\left[r_m(n)\right]}\right\}\right\} \end{aligned} \tag{43}$$

In order to show G_{im} is bounded, we need to prove that its real and imaginary part are bounded, respectively.

For any complex random variable $Y = Y_1 + jY_2$, we have

$$\mathrm{Re}\{Y\} \triangleq \mathrm{Re}\{Y_1 + jY_2\} = Y_1 \le |Y_1| \le \sqrt{Y_1^2 + Y_2^2} = |Y| \tag{44}$$

and

$$\mathrm{Re}\{E\{Y\}\}=\mathrm{Re}\{E\{Y_1+jY_2\}\}=E\{Y_1\}=E\{\mathrm{Re}\{Y\}\}. \quad (45)$$

Using (43) and (44), we can obtain

$$\begin{aligned}\mathrm{Re}\left\{G_{im}\right\} &= \mathrm{Re}\left\{E\left\{r_i\left(n\right)\frac{r_m^*\left(n\right)}{f\left[r_i\left(n\right)\right]f\left[r_m\left(n\right)\right]}\right\}\right\}\\ &= E\left\{\mathrm{Re}\left\{r_i\left(n\right)\frac{r_m^*\left(n\right)}{f\left[r_i\left(n\right)\right]f\left[r_m\left(n\right)\right]}\right\}\right\}\\ &\le E\left\{\left|r_i\left(n\right)\frac{r_m^*\left(n\right)}{f\left[r_i\left(n\right)\right]f\left[r_m\left(n\right)\right]}\right|\right\}\\ &= E\left\{\frac{\left|r_i\left(n\right)\right|}{\left|f\left[r_i\left(n\right)\right]\right|}\frac{\left|r_m^*\left(n\right)\right|}{\left|f\left[r_m\left(n\right)\right]\right|}\right\}.\end{aligned} \quad (46)$$

When $\left|r_i\left(n\right)\right| \le \zeta\left(n\right)$, we consider that $r_i\left(n\right)$ is not damaged by spike impulsive interference. We have

$$\mathrm{Re}\left\{G_{im}\right\}<\infty, \quad 0<\alpha<2 \quad (47)$$

When $\left|r_i\left(n\right)\right| > \zeta\left(n\right)$, $r_i\left(n\right)$ is affected by spike impulsive interference. According to (1) and (46), $E\left\{\frac{r_i(n)r_m^*(n)}{f[r_i(n)]f[r_m(n)]}\right\}$ can be expressed as in (48).

Let $X_1 = \tilde{s}_i\left(n\right) + \tilde{I}_i\left(n\right) + \tilde{w}_i\left(n\right)$ and $X_2 = \tilde{s}_m\left(n\right) + \tilde{I}_m\left(n\right) + \tilde{w}_m\left(n\right)$. For given $\tilde{s}_i\left(n\right)$ and $\tilde{s}_m\left(n\right)$, when SNR is a given constant and $I_i\left(n\right)$ and $I_m\left(n\right)$ are jointly $S\alpha S$, then X_1 and X_1 are jointly $S\alpha S$. If complex Y_1 and Y_1 are jointly $S\alpha S$ random variables, and $|\vartheta| > 0$, we have

$$E\left\{\frac{|Y_1|}{|Y_1|+|\vartheta|}\frac{|Y_2|}{|Y_2|+|\vartheta|}\right\}<\infty. \quad (49)$$

Based on the analysis in [30], the conditional expectation in (48) is bounded as (50).

According to (50) into (48), $\mathrm{Re}\left\{G_{im}\right\}$ is upper bounded, that is

$$\begin{aligned}\mathrm{Re}\{G_{im}\} &= E\left\{\mathrm{Re}\left\{\frac{r_i\left(n\right)}{|r_i\left(n\right)|+|\vartheta|}\frac{r_m^*\left(n\right)}{|r_m\left(n\right)|+|\vartheta|}\right\}\right\}\\ &\le E\left\{\frac{\left|r_i\left(n\right)\right|}{|r_i\left(n\right)|+|\vartheta|}\frac{\left|r_m^*\left(n\right)\right|}{|r_m\left(n\right)|+|\vartheta|}\right\}<\infty, \quad 1<\alpha<2\end{aligned} \quad (51)$$

Next, for any complex random variable $Y = Y_1 + jY_2$, we have the fact that

$$\mathrm{Re}\{Y\}\triangleq\mathrm{Re}\{Y_1+iY_2\}=Y_1\ge-\left|Y\right|. \quad (52)$$

Following the same procedure in (46), we obtain

$$\begin{aligned}\mathrm{Re}\left\{G_{im}\right\} &\ge -E\left\{\left|\frac{r_i\left(n\right)}{|r_i\left(n\right)|+|\vartheta|}\frac{r_m^*\left(n\right)}{|r_m\left(n\right)|+|\vartheta|}\right|\right\}\\ &= -E\left\{\left|\frac{r_i\left(n\right)}{|r_i\left(n\right)|+|\vartheta|}\right|\left|\frac{r_m^*\left(n\right)}{|r_m\left(n\right)|+|\vartheta|}\right|\right\}\\ &= -E\left\{\frac{\left|r_i\left(n\right)\right|}{|r_i\left(n\right)|+|\vartheta|}\frac{\left|r_m^*\left(n\right)\right|}{|r_m\left(n\right)|+|\vartheta|}\right\}.\end{aligned} \quad (53)$$

Substituting (51) into (53), we get

$$\mathrm{Re}\left\{G_{im}\right\} > -\infty, \quad 1<\alpha<2. \quad (54)$$

Overall, $\mathrm{Re}\left\{G_{im}\right\}$ is both upper and lower bounded, i.e.,

$$-\infty<\mathrm{Re}\left\{G_{im}\right\}<\infty, \quad 1<\alpha<2. \quad (55)$$

Similar to the above proof process, it can also be proved that the imaginary part is bounded. It should be noted that G_{im} is not a complex number in this paper. Therefore, the (i,m)-th entry G_{im} is bounded.

APPENDIX B
PROOF OF PROPOSITION 2

We first substitute $r_i\left(n\right)$ into the elements of the GCM G_{im}

$$\begin{aligned}G_{im} &= E\left\{\frac{r_i\left(n\right)r_m^*\left(n\right)}{f\left[r_i\left(n\right)\right]f\left[r_m\left(n\right)\right]}\right\}\\ &= E\left\{\frac{\sum_{q=1}^{M_t}h_{iq}s_q\left(n\right)+I_i\left(n\right)+w_i\left(n\right)}{f\left[r_i\left(n\right)\right]}\right.\\ &\left.\times\frac{\sum_{p=1}^{M_t}h_{mp}s_p\left(n\right)+I_m\left(n\right)+w_m\left(n\right)}{f\left[r_m\left(n\right)\right]}\right\}\end{aligned} \quad (56)$$

Because the transmitted signal $s_q\left(n\right)$, the interference $I_m\left(n\right)$ and the noise $w_m\left(n\right)$ are independent, (i,m)-th entry G_{im} can be further expressed as in (57).

According to the process in [30], the (i,m)-th entry G_{im} can be further simplified and approximately expressed as

$$\begin{aligned}G_{im}\simeq&\sum_{q=1}^{M_t}h_{iq}E\left\{\frac{s_q(n)\left(\sum_{q=1}^{M_t}s_q(n)+I_m(n)+w_m(n)\right)}{f\left[r_i\left(n\right)\right]f\left[r_m\left(n\right)\right]}\right\}h_{mq}\\ &+E\left\{\frac{(I_i(n)+w_i(n))\left(\sum_{q=1}^{M_t}h_{mq}s_q(n)+I_m(n)+w_m(n)\right)}{f\left[r_i\left(n\right)\right]f\left[r_m\left(n\right)\right]}\right\}\end{aligned} \quad (58)$$

Applying variable changes, The (i,m)-th entry G_{im} can be expressed as

$$G_{im}\simeq\sum_{q=1}^{M_t}h_{iq}\Sigma_{qq}h_{mq}^*+\varpi_w^2\delta_{im}, \quad (59)$$

where

$$\Sigma_{qm}\simeq\delta_{qm}E\left\{\frac{s_q\left(n\right)\left(\sum_{q=1}^{M_t}s_q(n)+I_m(n)+w_m(n)\right)}{f\left[r_i(n)\right]f\left[r_m(n)\right]}\right\}, \quad (60)$$

$$\varpi^2=E\left\{\frac{(I_i(n)+w_i(n))\left(\sum_{q=1}^{M_t}h_{mq}s_q(n)+I_m(n)+w_m(n)\right)}{f\left[r_i(n)\right]f\left[r_m(n)\right]}\right\} \quad (61)$$

in which δ_{qm} is the Kronecker delta. Based on (59), the GCM $\mathbf{G_r}$ is rewritten as

$$\mathbf{G_r} = \mathbf{H\Sigma H}^{\dagger} + \varpi^2\mathbf{I}. \quad (62)$$

$$\begin{aligned}\operatorname{Re}\left\{G_{im}\right\} &\leq E\left\{\frac{\left|r_i\left(n\right)\right|}{\left|r_i\left(n\right)\right|+\left|\vartheta\right|}\frac{\left|r_m^*\left(n\right)\right|}{\left|r_m\left(n\right)\right|+\left|\vartheta\right|}\right\}\\ &= E\left\{\frac{\left|\sum\limits_{q=1}^{M_t}h_{iq}s_q\left(n\right)+I_i\left(n\right)+w_i\left(n\right)\right|}{\left|r_m\left(n\right)\right|+\left|\vartheta\right|}\frac{\left|\sum\limits_{p=1}^{M_t}h_{mp}s_p\left(n\right)+I_m\left(n\right)+w_m\left(n\right)\right|}{\left|r_m\left(n\right)\right|+\left|\vartheta\right|}\right\}\\ &\simeq E_{s_1}E_{s_2|s_1}E_{s_3|s_1,s_2}\cdots E_{s_{M_t}|s_1,s_2,\cdots,s_{M_t-1}}E_{I_m,I_n|s_1,s_2,\cdots,s_{M_t}}\\ &\quad\left\{\frac{\left|\sum\limits_{q=1}^{M_t}h_{iq}s_q\left(n\right)+I_i\left(n\right)+w_i\left(n\right)\right|}{\left|r_i\left(n\right)\right|+\left|\vartheta\right|}\frac{\left|\sum\limits_{p=1}^{M_t}h_{mp}s_p\left(n\right)+I_m\left(n\right)+w_m\left(n\right)\right|}{\left|r_m\left(n\right)\right|+\left|\vartheta\right|}\right\}\end{aligned} \tag{48}$$

$$E_{w_m,w_n|s_1,s_2,\cdots,s_{M_t}}\left\{\frac{\left|\sum\limits_{q=1}^{M_t}h_{iq}s_q\left(n\right)+I_i\left(n\right)+w_i\left(n\right)\right|}{\left|r_i\left(n\right)\right|+\left|\vartheta\right|}\frac{\left|\sum\limits_{p=1}^{M_t}h_{mp}s_p\left(n\right)+I_m\left(n\right)+w_m\left(n\right)\right|}{\left|r_m\left(n\right)\right|+\left|\vartheta\right|}\right\}<\infty \tag{50}$$

$$\begin{aligned}G_{im} &= E\left\{\frac{r_i\left(n\right)r_m^*\left(n\right)}{f\left[r_i\left(n\right)\right]f\left[r_m\left(n\right)\right]}\right\}\\ &= E\left\{\sum_{q=1}^{M_t}h_{iq}s_q\left(n\right)\left\{\frac{\sum\limits_{p=1}^{M_t}h_{mp}s_p\left(n\right)+I_m\left(n\right)+w_m\left(n\right)}{f\left[r_i\left(n\right)\right]f\left[r_m\left(n\right)\right]}\right\}+I_i\left(n\right)\left\{\frac{\sum\limits_{p=1}^{M_t}h_{mp}s_p\left(n\right)+I_m\left(n\right)+w_m\left(n\right)}{f\left[r_i\left(n\right)\right]f\left[r_m\left(n\right)\right]}\right\}\right.\\ &\quad\left.+w_i\left(n\right)\left\{\frac{\sum\limits_{p=1}^{M_t}h_{mp}s_p\left(n\right)+I_m\left(n\right)+w_m\left(n\right)}{f\left[r_i\left(n\right)\right]f\left[r_m\left(n\right)\right]}\right\}\right\}.\end{aligned} \tag{57}$$

REFERENCES

[1] J. Hu, S. Yan, X. Zhou, F. Shu and J. Wang, "Covert communications without channel state information at receiver in IoT systems," *IEEE Internet Things J.*, vol. 7, no. 11, pp. 11103-11114, Nov. 2020.

[2] C. Lin, G. Han, J. Du, T. Xu, L. Shu and Z. Lv, "Spatiotemporal congestion-aware path planning toward intelligent transportation systems in software-defined smart city IoT," *IEEE Internet Things J.*, vol. 7, no. 9, pp. 8012-8024, Sept. 2020.

[3] Y. A. Eldemerdash, O. A. Dobre, and M. Oner, "A new deep-Q-learning-based transmission scheduling mechanism for the cognitive internet of things," *IEEE Internet Things J.*, vol. 5, no. 4, pp. 2375-2385, Aug. 2018.

[4] T. Li, J. Yuan and M. Torlak, "Network throughput optimization for random access narrowband cognitive radio internet of things," *IEEE Internet Things J.*, vol. 7, no. 9, pp. 1436-1448, Jun. 2018.

[5] M. Gao, Y. Li, O. A. Dobre and N. Al-Dhahir, "Joint blind identification of the number of transmit antennas and MIMO schemes using gerschgorin radii and FNN," *IEEE Trans. Wireless Commun.*, vol. 18, no. 1, pp. 372-387, Jan. 2019.

[6] M. Mohammadkarimi and O. A. Dobre, "Blind identification of spatial multiplexing and alamouti space-time block code via kolmogorov-smirnov (K-S) test," *IEEE Commun. Lett.*, vol. 8, no. 10, pp. 1711-1714, Oct. 2014.

[7] Y. A. Eldemerdash, O. A. Dobre, and M. Oner, "Signal identification for multiple-antenna wireless systems: achievements and challenges," *IEEE Commun. Surv. Tuts.*, vol. 18, no. 3, pp. 1524-1551, 3rd Quart. 2016.

[8] M. Mohammadkarimi, E. Karami, and O. A. Dobre, "A novel algorithm for blind detection of the number of transmit antenna," in *Proc. Cognitive Radio Oriented Wireless Networks*, Oct. 2015, pp. 441-450.

[9] O. Somekh, O. Simeone, Y. Bar-Ness, and W. Su, "Detecting the number of transmit antennas with unauthorized or cognitive receivers in MIMO systems," in *Proc. IEEE Mil. Commun. Conf.*, Oct. 2007, pp. 478-482

[10] M. Shi, Y. Bar-Ness, and W. Su, "Adaptive estimation of the number of transmit antennas," in *Proc. IEEE Mil. Commun. Conf.*, Oct. 2007, pp. 1-5.

[11] K. Hassan, C. N. Nzeza, R. Gautier, E. Radoi, M. Berbineau, and I. Dayoub, "Blind detection of the number of transmitting antennas for spatially-correlated MIMO systems," in *Proc. IEEE 11th Int. Conf. ITS Telecommun.*, Aug. 2011, pp. 458-462.

[12] M. R. Oularbi, S. Gazor, A. Aissa-El-Bey, and S. Houcke, "Enumeration of base station antennas in a cognitive receiver by exploiting pilot patterns," *IEEE Commun. Lett.*, vol. 17, no. 1, pp. 8-11, Jan. 2013.

[13] M. Mohammadkarimi, E. Karami, O. Dobre, and M. Win, "Number of transmit antennas detection using time-diversity of the fading channel," *IEEE Trans. Signal Process.*, vol. 65, no. 15, pp. 4031-4046, Aug. 2017

[14] T. Li, Y. Li, Y. Chen, Cimini. L and H. Zhang, "Hypothesis testing based fast-converged blind estimation of transmit-antenna number for MIMO systems," *IEEE Trans. Veh. Technol.*, vol. 67, no. 6, pp. 5084-5095, Jun. 2018.

[15] T. Li, Y. Li, Cimini. L and H. Zhang, "Estimation of MIMO transmit-

antenna number using higher-order moments-based hypothesis testing," *IEEE Wireless Commun. Lett.*, vol. 7, no. 2, pp. 258-261, Apr. 2018.

[16] E. Ohlmer, T. Liang and G. Fettweis, "Algorithm for detecting the number of transmit antennas in MIMO-OFDM systems: receiver integration," in *Proc. IEEE Veh. Technol. Conf.*, Sept. 2008, pp. 1-5.

[17] T. Li, Y. Li, Cimini. L and H. Zhang, "Blind estimation of transmit-antenna number for non-Cooperative multiple-input multiple-output orthogonal frequency division multiplexing systems," *IET Commun.*, vol. 11, no. 17, pp. 2637-2642, Dec. 2017.

[18] Y. Chen, "Suboptimum detectors for AF relaying with gaussian noise and $S\alpha S$ interference," *IEEE Trans. Veh. Technol.*, vol. 64, no. 10, pp. 4833-4839, Oct. 2015.

[19] Y. Chen, X. Yang, L. Huang, and H. So, "Robust frequency estimation in symmetric α stable noise," *Circuits Syst. Signal Process.*, vol. 37, no.10, pp. 4637-4650, Oct. 2018.

[20] A. Mahmood, M. Chitre and M. A. Armand, "On single-carrier communication in additive white symmetric alpha-stable noise," *IEEE Trans. Commun.*, vol. 62, no. 10, pp. 3584-3599, Oct. 2014.

[21] G. Yang, J. Wang, G. Zhang, and S. Li, "Communication signal pre-processing in impulsive noise: a bandpass myriad filtering-based method," *IEEE Commun. Lett.*, vol. 22, no. 7, pp. 1402-1405, Jul. 2018.

[22] X. Yan, G. Liu, H. Wu, G. Zhang, Q. Wang and Y. Wu, "Robust modulation classification over α-stable noise using graph-based fractional lower-order cyclic spectrum analysis," *IEEE Trans. Veh. Technol.*, vol. 69, no. 3, pp. 2836-2849, Mar. 2020.

[23] J.G. Gonzalez, J.L. Paredes and G.R. Arce, "Zero-order statistics: a mathematical framework for the processing and characterization of very impulsive Signals," *IEEE Trans. Signal Process.*, vol. 54, no. 10, pp. 3839-3851, Oct. 2006.

[24] W. Liu, P. P. Pokharel and J. C. Principe, "Correntropy: Properties and Applications in Non-Gaussian Signal Processing," *IEEE Trans. Signal Process.*, vol. 55, no. 11, pp. 5286-5298, Nov. 2007.

[25] J. Zhang, N. Zhao, M. Liu, C. Qian, Y, Chen, F. Gong and F. R. Yu, "Blind parameter estimation of M-FSK signals in the presence of alpha-stable noise," *IEEE Trans. Commun.*, vol. 68, no. 12, pp. 7647 - 7659, Dec. 2020.

[26] D. Huang, C. Wang, J. Wu, J. Lai and C.K. Kwoh, "Ultra-scalable spectral clustering and ensemble clustering," *IEEE Trans. Knowl. Data Eng.*, vol. 32, no. 6, pp. 1212-1226, Jun. 2020.

[27] A. B. Ayed, M. B. Halima and A. M. Alimi, "Adaptive fuzzy exponent cluster ensemble system based feature selection and spectral clustering," in *Proc. IEEE Int. Conf. Fuzzy Syst.*, Jul. 2017, pp. 1-6.

[28] Y. Shen, W. Pedrycz, Y. Chen, X. Wang and A. Gacek, "Hyperplane division in fuzzy C-means: Clustering Big Data," *IEEE Trans. Fuzzy Syst.*, vol. 28, no. 11, pp. 3032-3046, Nov. 2020.

[29] F. Nie, Z. Zeng, I. W. Tsang, D. Xu and C. Zhang, "Spectral embedded clustering: a framework for in-sample and out-of-sample spectral clustering," *IEEE Trans. Neural Netw.*, vol. 22, no. 11, pp. 1796-1808, Nov. 2011.

[30] T. H. Liu and J.M. Mendel, "A subspace-based direction finding algorithm using fractional lower order statistics," *IEEE Trans. Signal Process.*, vol. 49, no. 8, pp. 1605-1613, Aug. 2001.